STRUCTURAL AND NUMERICAL IDENTIFIABILITY OF THERMAL RESISTANCES IN PLATE FIN-AND-TUBE HEAT EXCHANGERS USING MANUFACTURER CATALOG DATA

Fernando Domínguez Muñoz[1*], Celestino R. Ruivo[2,3], José Manuel Cejudo López[4], Antonio Carrillo Andrés[4], Francisco Fernández Hernández[4]

1: Grupo Energética, Escuela de Ingenierías Industriales, Universidad de Málaga
Calle Dr. Ortiz Ramos s/n, 29071, Málaga, Spain
email: fdominguezm@uma.es

2: Department of Mechanical Engineering, Institute of Engineering, University of Algarve,
Faro, 8005-139, Portugal
email: cruivo@ualg.pt

3: ADAI-LAETA, Department of Mechanical Engineering, University of Coimbra
Coimbra, 3030-788, Portugal
email: cruivo@ualg.pt

4: Grupo Energética, Escuela de Ingenierías Industriales, Universidad de Málaga
Calle Dr. Ortiz Ramos s/n, 29071, Málaga, Spain
email: {jmcejudo, acarrillo, franciscofh}@uma.es

Abstract: *Plate fin-and-tube heat exchangers, commonly known as heating/cooling coils, are widely used in HVAC systems to transfer heat to or from air. A problem of practical interest in coil simulation is to identify the thermal resistances on the air and liquid sides using manufacturer catalog data. Manufacturers rarely provide detailed information (geometry and circuitry) of the coils they sell or install in factory-made equipment such as air handling units or fan-coils; they just report the performance of the coil at a few typical operating conditions. This paper examines whether it is mathematically possible to back-calculate the thermal resistances on the air and liquid sides using a set of performance data that is disturbed by noise (e.g. measurement errors) and consists of operating cases in which none of the two thermal resistances can be neglected. The first part of the paper discusses the structural identifiability problem, that is, the mathematical possibility of fitting Nusselt-type correlations for air and liquid, as well as a constant resistance for the wall. The second part of the paper discusses the possibility of calculating the numerical value of the parameters of the Nusselt correlations (constant or constant and exponent) using noisy data. The analysis is applied to a typical coil, which is simulated by means of a mathematical model.*

Keywords: Heat exchanger, coil, thermal resistance, identifiability

1. INTRODUCTION

The thermal performance of a heat exchanger depends on three main factors: (1) size and geometry of the heat exchanging surface, (2) average temperature difference between the heat exchanging fluids, and (3) thermal resistance between these fluids. When all physical and operational characteristics of a heat exchanger are known, detailed models can be used to predict its duty and effectiveness accurately. However, constructive details are rarely available from manufacturer catalogues, which only quote the capacity and pressure losses for a few selected conditions defined by combinations of flow rates and inlet and outlet temperatures. Furthermore, catalog data is inevitably affected by some degree of uncertainty associated to the procedure by which the data was obtained. Catalogues are produced using laboratory tests and/or proprietary software. In both cases, the nominal tolerances on the declared capacities range from 5% to 20% depending on the market, application and manufacturer.

The engineer thus faces the challenge of simulating a heat exchanger with minimal and, to some extent, noisy information. For the sake of simplicity, in this paper we will restrict our attention to air–water coils operating in dry regime (no condensate on the air side), which is an interesting case to study because of the large difference between the air and water thermal resistances. The information available on the coil catalog consists of a set of $k = 1,\ldots,N$ operating points, each of them defined by the following data: Q_k, $m_{a,k}$, $T_{a,in,k}$,

$m_{w,k}$, $T_{w,in,k}$ where Q_k is the transferred heat, $m_{a,k}$ is the air mass flowrate, $T_{a,in,k}$ is the air inlet temperature, $m_{w,k}$ is the liquid mass flowrate, and $T_{w,in,k}$ is the liquid inlet temperature. The goal is to use this information to calculate the performance of the heat exchanger in any other conditions. This calculation comprises three basic steps:

1. The appropriate ε–NTU equation or numerical model is used to calculate the overall thermal resistance (R_T) on each of the N known points
2. The data obtained in the previous step is used to fit a model for R_T, i.e., a mathematical expression that let us to calculate the thermal resistance for any values of $m_{a,k}$, $T_{a,k}$, $m_{w,k}$, $T_{w,k}$ (temperatures here would be average or caloric)
3. The appropriate ε–NTU equation or numerical model is used along with the fitted function for R_T to calculate the performance at the desired conditions.

Note that steps 1 and 3 require knowing the flow configuration of the heat exchanger. Pure counter-current flow or pure cross-current flow are usually assumed when no information is available, see for example Wetter [1] or Lemort [2]. Note also that step 2 requires splitting the overall resistance into air and water resistances. The standard experimental procedure to measure the air thermal resistance is to make it much larger than the water resistance, or alternatively calculate the water resistance using a recognized correlation. This is not the case when catalog data is used: the engineer neither knows the order of magnitude of the resistances nor the water velocity to calculate the liquid resistance. Some authors use a single operating point (N=1) and assume a fixed air to liquid resistance ratio, see for example Wetter [1] or Vera-García [3]. Others such as Rabehl [4] or Ruivo [5,6] use several catalog points (N≥2) and fit a model for R_T.

This paper investigates whether it is mathematically possible to identify the different thermal resistances of a finned heat exchanger using limited amount of data affected by measurement errors, and in which none of the thermal resistances is necessarily dominant. Previous work [1-6] tend to judge the success of the procedure by the prediction ability of the identified model (step 3), while the accuracy of the identified resistances (step 2) is rarely questioned beyond a basic order of magnitude check. This paper focuses on the latter problem, analyzing the variance in the different parameters that appear in the R_T correlating function.

2. THERMAL RESISTANCES IN A HEAT EXCHANGER

The overall resistance of a heat exchanger can be split into three resistances in series: convective resistance on the air side (R_A), conductive resistance of the heat exchanger metal (R_M), and convective resistance on the liquid side (R_L):

$$R_T = R_A + R_M + R_L \,. \tag{1}$$

The above expression can be further written as:

$$R_T = \frac{1}{\left(A_{PA} + \eta A_{EA}\right) h_A} + R_M + \frac{1}{A_L h_L}, \tag{2}$$

where A_{PA} is the air-side tube area not occupied by fins, η is the fin efficiency, A_{EA} is the air-side extended surface, h_A is the air-side convection coefficient, A_L is the total liquid-side heat transfer area, and h_L is the liquid-side convection coefficient. For forced convection, a correlation of the following type is usually assumed:

$$Nu = C \cdot Re^n \cdot Pr^m \tag{3}$$

The exponent n depends on the type of flow, with n=0,6 for laminar flow and n=0,8 for turbulent flow. For the exponent m, a value of 0,4 can be used when the fluid is heating up ($T_{surface}>T_{fluid}$) and a value of 0,3 is used in the opposite case. Expanding the dimensionless numbers in Equation (3), the convection coefficient can be written as:

$$h = \underbrace{C\left(\frac{L_c^{n-1}}{A_{cr}^n}\right)}_{C^*} \underbrace{\left(\mu^{m-n} c_p^m k^{1-m}\right)}_{P^*} \dot{m}^n = C^* P^* \dot{m}^n \tag{4}$$

where L_c is the characteristic length of the geometry (inner diameter for liquid, collar diameter for air), A_{cr} is the cross section area (minimum flow area in the case of the air), μ is the dynamic viscosity, k is the thermal conductivity, and c_p is the specific heat. These properties are evaluated at the caloric temperature of the fluid.

It is interesting to note that all geometrical parameters can be lumped along with C into a single constant C^*, while all thermal properties (which depend on temperature and pressure) can be lumped into a single group P^*. For a given coil geometry C^* will be constant, while the influence of P^* on h will depend on the fluid and the range in which temperatures vary. In the case of air conditioning applications, the largest variations in P^* occur on the liquid side. For example, for water at atmospheric pressure, n=0,6 and m = 0,3, P^* varies 36,5% between 30ºC and 60ºC. For air, the variation in the same conditions is just of 3,5%. Substituting (4) into (2) and lumping all multiplying factors into the parameters a and c:

$$R_T = \frac{1}{C_A^* P_A^* \dot{m}_A^b} + R_M + \frac{1}{C_L^* P_L^* \dot{m}_L^d} = a\dot{m}_A^{-b} + R_M + c\dot{m}_L^{-d}, \quad (5)$$

3. METHODOLOGY

The problem of interest is the possibility of identifying a, b, c, d and R_M in Equation (5) using N known values of R_T, $m_{a,k}$, $T_{a,k}$, $m_{w,k}$, $T_{w,k}$. The following assumptions will be made:

1. To focus on the identification problem alone, it will be supposed that the true flow configuration of the heat exchanger was used in reducing R_T from catalog data. In a real situation the flow configuration is unknown, which introduces additional bias in the estimates of R_T
2. For reasons of space, the effects of temperature on Equation (5) will not be considered. That is, it will be assumed that all N points used in the calculations share the same average temperatures for water and air, so that the only independent variables in (5) will be the mass flowrates. The calculations presented below are easily extended to include m in Equation (4) as an additional parameter to fit
3. One important limitation of simple models is that there are no single exponents b, c in Eq. (5) valid over the whole operating range of the heat exchanger. With no information about geometry and circuitry of the coil, it is impossible to determine the critical flowrates at which regime transitions occur in a particular coil. In the following sections, mass flowrates will be varied in the appropriate ranges that keep the liquid in turbulent regime and the air in laminar regime, which are by far the most prevalent operating conditions.

Two separate issues must the analyzed to determine if the empirical constants in Equation (5) can be estimated: the structural identifiability of the model parameters themselves (Section 3.1) and the possibility of calculating their numerical values with low bias and low variance (Section 3.2).

3.1. Structural identifiability

Structural identifiability is the problem of investigating the conditions under which system parameters of a model can be uniquely determined from experimental data, no matter how noise-free the measurements. This condition can be detected by analyzing the model equations. To illustrate the idea, consider the trivial model $y = (a+b)\cdot x$, where a and b are the parameters to identify, x is the input variable and y is the response. It is clear that a and b cannot be independently determined from (x, y) measurements, no matter the number and quality of these measurements. At best, only the overall term (a+b) can be identified.

The sensitivity coefficient approach, demonstrated by Beck [7], provides a formal method to test the structural identifiability of a model. Consider a model y (x, p) where $x = \{x_1, x_2, \ldots, x_r\}$ are r independent variables and $p = \{p_1, p_2, \ldots, p_q\}$ are q parameters to estimate. Let k be one of the N observations (catalog data points). The condition of structural identifiability is that the sensitivity coefficients of y with respect to p_j ($\partial y/\partial p_j$) should be linearly independent over the range of the observations. This condition implies that no set of constants C_i ($\neq 0$) exists such that:

$$C_1 \frac{\partial y_k}{\partial p_1} + C_2 \frac{\partial y_k}{\partial p_2} + \ldots + C_q \frac{\partial y_k}{\partial p_q} = 0 \quad \forall k = 1 \ldots N . \quad (6)$$

Note that the condition (6) must hold true for all N observations (catalog points).

3.2. Numerical identifiability

Data used in the parameter estimation will be inevitably affected by measurement errors. Even when the model is structurally identifiable and the errors are low, it may be not possible to identify the parameters without bias or minimum variance due to one or several of the following problems:

1. Improper or under-parametrized model that does not represent the physics of the system
2. Over-parametrized model, with more independent variables than needed, which can lead to multi-collinearity effects between regressor variables
3. Improper sampling, typically due to poor covering of the domain or inadequate richness of the data in a narrow region of the domain
4. Large sensitivity of some parameters to measurement errors
5. Etc.

Regarding point 1, it was already discussed that our model, equation (5), cannot represent regime transitions. If the regression is performed using a dataset including laminar and turbulent conditions, the estimated parameters will poorly describe the coil behavior. Furthermore, although forced convection correlations follow the general format of Equation (3), they tend to be much more detailed, see for example Kim's correlation for h_a [9]. Thus, our model does not fully capture some of the physical phenomena. Regarding point 3, data used in the identification process must cover a domain wide enough to capture how R_T varies with m_a and m_w (see figure 2 for that purpose). In this paper, we will suppose this is the case. However, printed catalogs tend to quote just 3 or 4 operating points for different air mass flowrates (fan speeds), which can be insufficient. Regarding point 4, intuition suggest that the water-side thermal resistance of a coil must be harder to identify that the air-side thermal resistance. The latter is much larger and dominates the heat transfer process. As we will see in Sections 4 and 5, this is the case.

From the previous discussion, we see there are many possible sources of variance in the estimated parameters. Each of them merits its own analysis. However, the essence of the problem can be tackled in an easy way with the help of the conceptual experiment depicted in Figure 1. In this theoretical exercise, we will suppose that we know the "true" values of the parameters *a*, *b, c, d*. From these parameters, the corresponding "true" values of R_T can be calculated at the discrete points of a (m_a, m_w) mesh covering the domain of interest. The important point here is that these true values of R_T are hidden from the experimenter, whose measurements will always contain some random measurement errors. The measurement process can be simulated using the Monte Carlo method: (1) random errors are generated by drawing random numbers from the appropriate probability distributions so as to mimic our understanding of the underlying process and measurement errors, (2) synthetic experiments can be constructed by disturbing the "true" value of R_T with the generated synthetic errors: $R_{T,measured} = R_{T,true}*error$. Each of these Z experiments represents a possible realization of the true parameters in the "real world". For each experiment, a new set of parameters *a*, *b, c, d* can be fitted. The resulting set of Z fitted parameters can then be statistically analyzed, providing valuable information on the range of variation of the identified parameters.

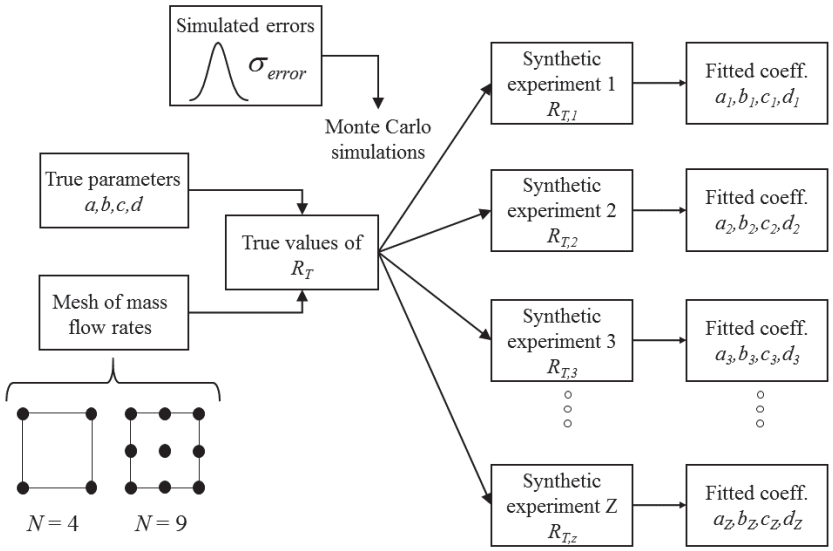

Figure 1. Monte Carlo simulation of and experiment

4. CASE STUDY

To perform the experiment proposed in Section 3, realistic values for the "true" parameters *a*, *b, c, d* are needed. A typical heating coil will be used as a test case, whose main characteristics are summarized in

Table 1. A mathematical model was developed to simulate the thermal performance of this coil. The 3 pass mixed cross-counter flow configuration of the coil was simulated using the ε–NTU equations "SERP-CU-3,4" as given in Reference [8]. The air-side convection coefficient was calculated using the Kim [9] correlation, and the water-side convection coefficient in the turbulent regime was calculated using the Gnielinski correlation [10]. In the transition region, the water–side Nusselt number was linearly interpolated between the Nusselt values corresponding to Re = 2300 (upper limit of laminar region) and Re = 10000 (lower limit of turbulent region). For copper tubes with collared fins, the wall and contact resistances are negligible, so they have not been included in the calculations. The model results were compared with the results of a certified software provided by the manufacturer "DBM Coils". Relative differences in the calculated capacity were within a 4% band for a wide range of operating conditions.

Table 1. Example coil characteristics

Number of tube rows in the air flow direction	3
Number of tubes on each row	30
Number of circuits	10
Length of a tube (one pass)	1500 mm
Outer diameter of a tube	12.5 mm
Thickness of the tube wall	0.4 mm
Center-to-center tube spacing in air flow direction	26 mm
Center-to-center tube spacing transverse to air flow direction	30 mm
Fin density	400 fins/m
Fin thickness	0.2 mm
Fin conductivity	234.5 W/m·K

The geometric areas in Equation (2) for this coil are: A_{PA} = 5.014 m^2, A_{EA} = 70.487 m^2, A_L = 4.941 m^2. The nominal mass flowrates can be chosen by fixing typical velocities for each fluid: m_a = 4 kg/s for a front air velocity of 2.5 m/s and m_L = 1.6 kg/s for a water velocity of 1.5 m/s. For these mass flow rates and assuming caloric temperatures of 20ºC for air and 50ºC for water, the calculated convection coefficients are h_a = 62.4 W/m^{2}K (Re_a = 4034) and h_L = 9164 W/m^{2}K (Re_L = 29449). The resulting fin effectiveness, calculated using the Schmidt formula, is η =0.88. Taking b = *–0.6* (laminar flow for air) and d = –0.8 (turbulent flow for water), the following constants are obtained: a = 0.549 and c = 0.03217. These results just represent a physically plausible set of values for the parameters that can be used in the hypothetical experiment proposed in Section 3. The resulting R_T surface is represented in Figure 2, were the mass flow rates have been varied within a [50%,150%] range around the nominal values. From this figure, it is apparent the much larger influence of m_a on R_T over the whole domain (note the slopes on each coordinate).

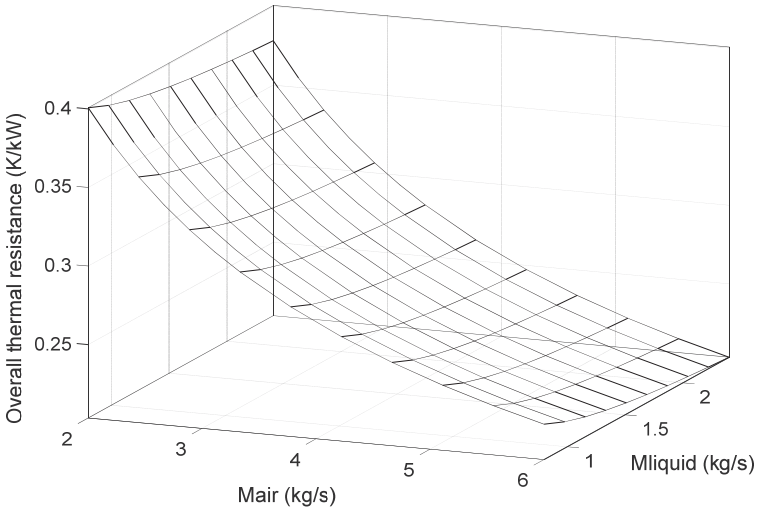

Figure 2. Overall thermal resistance surface for the case study

5. RESULTS AND DISCUSSION

The methodology outlined in Section 3 is now applied to the case study of Section 4. In some references [2,5,6] the value of the exponents in Equation (5) is assumed and the experimental data is used to fit the parameters *a* and *c*. In other cases [4-6], all four parameters are attempted to be fitted from experimental data. Both options will now be analyzed in terms of the possibility of identifying the parameters and calculate their values with enough accuracy.

5.1. Structural identifiability

Let us apply the structural identifiability condition (6) to the model (5). The parameters in the model will be identifiable if the sensitivity coefficients are linearly independent, i.e., if no set of constants C_i exists such that

$$C_1 \frac{\partial R_{T,i}}{\partial a} + C_2 \frac{\partial R_{T,i}}{\partial b} + C_3 \frac{\partial R_{T,i}}{\partial c} + C_4 \frac{\partial R_{T,i}}{\partial d} + C_5 \frac{\partial R_{T,i}}{\partial R_m} = 0\,, \tag{6}$$

for all observations $i = 1$ to N and for not all the C_j equal to zero. Calculating the derivatives in (6), we obtain:

$$C_1 \dot{m}_{A,i}^{-b} - C_2 a \dot{m}_{A,i}^{-b} \ln\left(\dot{m}_{A.i}\right) + C_3 \dot{m}_{L.i}^{-d} - C_4 c \dot{m}_{L,i}^{-d} \ln\left(\dot{m}_{L,i}\right) + C_5 = 0\,. \tag{7}$$

In the particular case in which the exponents are known, equation (6) reduces to:

$$C_1 \dot{m}_{A,i}^{-b} + C_3 \dot{m}_{L,i}^{-d} + C_5 = 0\,. \tag{8}$$

When the wall resistance is neglected, $C_5 = 0$ in (7) and (8). In general, no set of non-trivial constants C_i exists that makes (7) or (8) zero for all observations. It follows that all parameters in the model (5) are structurally identifiable. Only very special cases can lead to identifiability problems, for example if $b = d$ and both mass flowrates are very similar ($m_{a,i} \approx m_{L,i}$), equation (8) can hold for $C_1 = 1$, $C_2 = -1$ and $C_5 = 0$, which makes the sensitivity coefficients linearly dependent and indicates identifiability problems. However, these operating conditions are very unusual for a coil.

5.2. Numerical identifiability for known exponents

Let us suppose that the experimenter imposes $b = -0,6$ (laminar air) and $d = -0,8$ (turbulent liquid) before fitting the experimental data. The wall resistance is neglected. The problem reduces to determine *a* and *c*. Applying the method outlined in Figure 1, we can simulate as many experiments as desired. Figure 1 shows the result of one of these simulations, performed under the following conditions: normally distributed measurement errors with $\sigma_{error} = 0.05$ (10% for 2σ), $N = 9$ points (generated by combining three flowrates per fluid: 0,5*nominal, nominal and 1,5*nominal), and $Z = 1000$ synthetic experiments. Each point in Figure 3 represents the outcome of one of these virtual experiments. Depending on the particular distribution of the random errors, the calculated values of *a* and *c* vary for each test. Figure 3 shows the whole range of possible results that we can expect in practice. The histogram of each variable is drawn on the margin. Note that the average values of *a* and *c* are very close to the true ones, but the result of a single experiment can be far away.

Table 2 represents the average and standard deviation of the probability distribution of the identified parameters (a, c) for different error levels (σ_{error}) and number of points employed (N). Two important conclusions are apparent:

1. The relative variance (σ/μ) in *c* is always much larger that in *a*. This means that it is very hard to identify the liquid thermal resistance, even for very low levels of measurement error. This result can be easily understood geometrically by looking at Figure 1: the dominant slope in the R_T surface is that associated to m_a. When the R_T data used to interpolate this surface is affected by moderate measurement errors, so that points do not exactly lie on the surface, the smaller slope will be much easier affected. The larger slope is dominant and much more immune to changes in the position of the data points.
2. As clearly shown in Figure 3, *a* and *c* are strongly negatively correlated (the coefficient of correlation is around $\rho = -0,9$ for all cases in Table 2). This means that larger–than–average values of

a are typically paired with smaller–than–average values of *c*. In some cases, *c* is even negative, which is non-sense. When *a* takes a large value, it can be said that it has usurped more than its appropriate share of explicative power of R_T in detriment of c, which has to correct itself to such a degree that it ends up assuming a negative value (in some cases) and a negative correlation (in all cases).

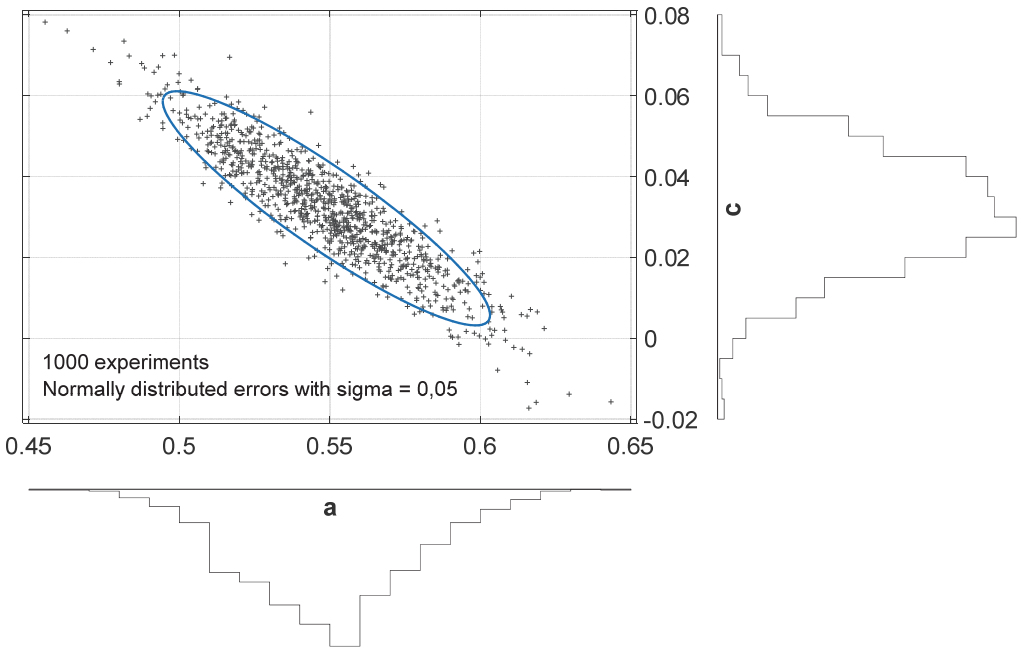

Figure 3. Set of possible outcomes of 1000 different experiments, along with histograms for *a* and *c*

Table 2. Mean value and standard deviation in identified parameters for different levels of experimental error and number of points used in the identification process (*N*), case of known exponents

N	Param.	True value	σ_{error}= 0.025			σ_{error}= 0.05			σ_{error}= 0.1		
			μ	*σ*	*σ/μ*	*μ*	*σ*	*σ/μ*	*μ*	*σ*	*σ/μ*
4	**a**	0.549	0.549	0.0168	3.06%	0.5489	0.0337	6.14%	0.5489	0.0673	12.26%
	c	0.0322	0.032	0.0085	26.56%	0.0318	0.0169	53.14%	0.0313	0.0338	107.99%
9	**a**	0.549	0.5486	0.0129	2.35%	0.5483	0.0258	4.71%	0.5476	0.0516	9.42%
	c	0.0322	0.0323	0.0068	21.05%	0.0323	0.0135	41.80%	0.0325	0.0271	83.38%
16	**a**	0.549	0.5491	0.0109	1.99%	0.5491	0.0218	3.97%	0.5493	0.0436	7.94%
	c	0.0322	0.0321	0.0058	18.07%	0.032	0.0116	36.25%	0.0317	0.0232	73.19%

5.3. Numerical identifiability for unknown exponents

In this case, the calculation process is identical to the one previously described, with the only difference that two additional parameters are included in the fitting calculations (*b* and *d*), which now become non-linear. In this case, the resulting probability distributions for the parameters and are far from normal. For this reason, in Table 3 we quote the average value of each parameter and the 10% and 90% percentiles of its distribution. The search space was limited to [–2,2] for all variables, and the solver not always converged to a solution. For this reason, a large number of simulations were run (≈10000) for each case in Table 3, an only those simulations that converged were used in the calculations. An additional column has been including, showing the maximum deviation Δ/μ where $\Delta = max(P_{90\%} - \mu, \mu - P_{10\%})$.
Regarding the correlation between variables, results show a very strong negative correlation between *c* and *d,* and no significant correlation between the rest of variables. Variance levels have largely increased compared to Table 2.

Table 3. Mean value and percentiles of identified parameters for different levels of experimental error and number of points used in the identification process (*N*), case of unknown exponents

N	Coef.	True values	σ_{error}= 0.025				σ_{error}= 0.1			
			$P_{10\%}$	μ	$P_{90\%}$	Δ/μ	$P_{10\%}$	μ	$P_{90\%}$	Δ/μ
9	**a**	0,549	0,51896	0,54822	0,57360	5,34%	0,47808	0,62217	0,75540	23,16%
	b	0,6	0,54856	0,64665	0,87405	35,17%	0,47018	0,83383	1,80951	117,01%
	c	0,0322	0,01191	0,04117	0,11379	176,40%	-0,00580	0,02494	0,19691	689,51%
	d	0,8	0,18783	1,35643	2,00000	86,15%	0,04988	1,27649	2,00000	96,09%
16	**a**	0,549	0,52023	0,54733	0,56981	4,95%	0,48835	0,60445	0,70960	19,21%
	b	0,6	0,55136	0,63518	0,82298	29,57%	0,49198	0,82113	1,64067	99,80%
	c	0,0322	0,01299	0,03974	0,10262	158,21%	0,00534	0,03871	0,19275	397,97%
	d	0,8	0,20741	1,29716	2,00000	84,01%	0,06847	1,25734	2,00000	94,55%

6. CONCLUSIONS

The results presented in Section 5.1 show that all parameters in Equation (5) are theoretically identifiable using catalog data. However, when it comes to calculate their numerical values, it is found that it is very difficult to split the total thermal resistance into air and water terms. Two effects complicate this task: (**1**) water-side related parameters (*c* and *d*) are very sensitive to measurement errors; normally the dominant thermal resistance is that of the air-side, (**2**) different variables can compete among them for explaining the data, appearing negative cross-correlations. For the case study outlined in the paper, the estimates are much better when the exponents in Equation (5) are given physically reasonable values, instead of trying to adjust them. Although the methodology used in the paper relies on a simple conceptual experiment, it is useful because it provides valuable insight into the problem. Using real catalog data will only make matters worse, amplifying the effects that are observed in our experiment: unknown flow configuration, larger measurement errors, less data points, points with mixed regimes, temperature effects, etc. will all contribute to increase the variances observed in our analysis.

REFERENCES

[1] Wetter M. Simulation Model. Finned Water-to-Air Coil without Condensation. Simulation Research Group, Lawrence Berkeley National Laboratory. January 1999. Report available at: https://simulationresearch.lbl.gov/dirpubs/42355.pdf

[2] Lemort V, Cuevas C, Lebrun J, Teodorese IV. Development of simple cooling coil models for simulation of HVAC systems. ASHRAE Transactions, 2008, Vol. 114 Issue 1, 319-328

[3] Vera-García F, García-Cascales JR, Gonzálvez-Maciá J, Cabello R, Llopis R, Sanchez D, Torrella E. A simplified model for shell-and-tubes heat exchangers: practical application. Applied Thermal Engineering 2010, 30:1231-1241.

[4] Rabehl RJ, Mitchell JW, Beckman WA. Parameter estimation and the use of catalog data in modeling heat exchangers and coils. HVAC&R Research 1999, 5:3-17

[5] Ruivo CR, Domínguez-Muñoz F, Costa JJ. Simplified model of finned-tube heat exchangers based on the effectiveness method and calibrated with manufacturer and experimental data. Applied Thermal Engineering 2017, 111:340-352.

[6] Ruivo CR, Domínguez-Muñoz F, Costa JJ, Fernández-Hernández F. Accuracy of simplified heating coil models based on manufacturer catalogue data. Thermal Science and Engineering Progress, 2017, 3:10-23.

[7] Beck JV, Arnold KJ. Parameter Estimation in Engineering and Science. Wiley 1977

[8] ESDU. Design and Performance Evaluation of Heat Exchangers: The Effectiveness – NTU Method. PART 3: Graphical and Analytical Data.

[9] Kim NH, Youn B, Webb RL. Air-Side Heat Tranfer and Friction Correlations for Plain Fin-and-Tube Heat Exchangers With Staggered Tube Arragements. Transactions of the ASME, Vol. 121, pp. 662 – 667, August 1999

[10] Verein Deutscher Ingenieure, VDI-Gesellschaft Verfahrenstechnik und Chemieingenieurwesen. VDI Heat Atlas, Chapter G1. Springer-Verlag 2010